4.6

Color and Multispectral Image Representation and Display

H.J. Trussell
North Carolina State University

1 Introduction

One of the most fundamental aspects of image processing is the representation of the image. The basic concept that a digital image is a matrix of numbers is reinforced by virtually all forms of image display. It is another matter to interpret how that value is related to the physical scene or object that is represented by the recorded image and how closely displayed results represent the data obtained from digital processing. It is these relationships to which this chapter is addressed.

Images are the result of a spatial distribution of radiant energy. The most common images are two-dimensional color images seen on television. Other everyday images include photographs, magazine and newspaper pictures, computer monitors and motion pictures. Most of these images represent realistic or abstract versions of the real world. Medical and satellite images form classes of images where there is no equivalent scene in the physical world. Because of the limited space in this chapter, we will concentrate on the pictorial images.

The representation of an image goes beyond the mere designation of independent and dependent variables. In that limited case, an image is described by a function

$$f(x, y, \lambda, t) \tag{1}$$

where x, y are spatial coordinates (angular coordinates can also be used), λ indicates the wavelength of the radiation and t represents time. It is noted that images are inherently two-dimension spatial distributions. Higher dimensional functions can be represented by a straightforward extension. Such applications include medical CT and MRI, as well as seismic surveys. For this chapter, we will concentrate on the spatial and wavelength variables associated with still images. The temporal coordinate will be left for another chapter.

In addition to the stored numeric values in a discrete coordinate system, the representation of multidimensional information includes the relationship between the samples and the real world. This relationship is important in the determination of appropriate sampling and subsequent display of the image.

Before presenting the fundamentals of image presentation, it is necessary to define our notation and to review the prerequisite knowledge that is required to understand the following material. A review of rules for the display of images and functions is presented in Section 2, followed by a review of mathematic preliminaries in Section 3. Section 4 will cover the physical basis for multidimensional imaging. The foundations of colorimetry are reviewed in Section 5. This material is required to lay a foundation for a discussion of color sampling. Section 6 describes multidimensional sampling with concentration on sampling color spectral signals. We will discuss the fundamental differences between sampling the wavelength and spatial dimensions of the multidimensional signal. Finally, Section 7 contains a mathematic description of the display of multidimensional data. This area is often neglected by many texts. The section will emphasize the requirements for displaying data in a fashion that is both accurate and effective. The final Section briefly considers future needs in this basic area.

2 Preliminary Notes on Display of Images

One difference between 1D and 2D functions is the way they are displayed. One-dimensional functions are easily displayed in a graph where the scaling is obvious. The observer need only examine the numbers which label the axes to determine the scale of the graph and get a mental picture of the function. With two-dimensional scalar-valued functions the display becomes more complicated. The accurate display of vector-valued two-dimensional functions, e.g., color images, will be discussed after covering the necessary material on sampling and colorimetery.

Two-dimensional functions can be displayed in several different ways. The most common are supported by MATLAB [1]. The three most common are the isometric plot, the gray scale plot and the contour plot. The user should choose the right display for the information to be conveyed. Let us consider each of the three display modalities. As simple example, consider the two-dimensional Gaussian functional form

$$f(m, n) = sinc\left(\frac{m^2}{a^2} + \frac{n^2}{b^2}\right)$$

where, for the following plots, $a = 1$ and $b = 2$.

The isometric or surface plots give appearance of three-dimensional drawing. The surface can be represented as a wire mesh or as a shaded solid, as in Fig. 1. In both cases, portions of the function will be obscured by other portions, for example, one can't see through the main lobe. This representation is reasonable for observing the behavior of mathematic functions, such as, point spread functions, or filters in the space or frequency domains. An advantage of the surface plot is that it gives a good indication of the values of the function since a scale is readily displayed on the axes. It is rarely effective for the display of images.

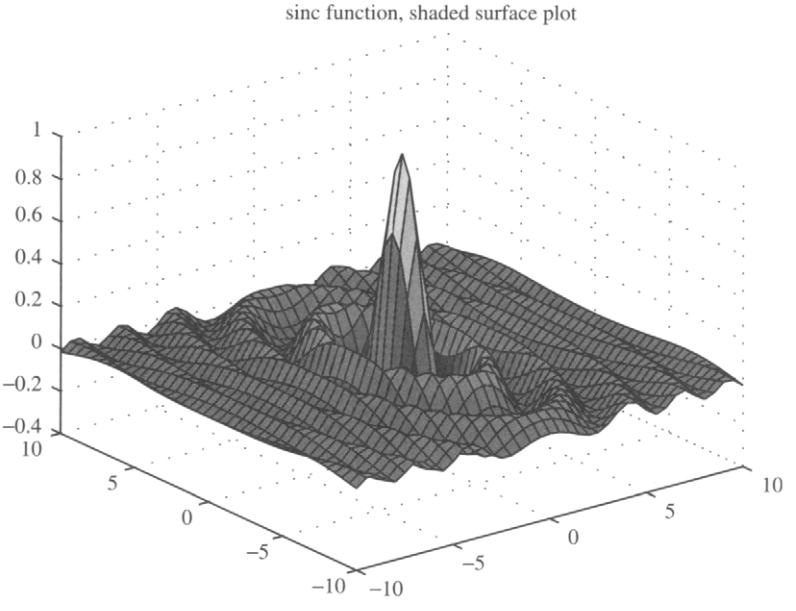

FIGURE 1 Shaded surface plot.

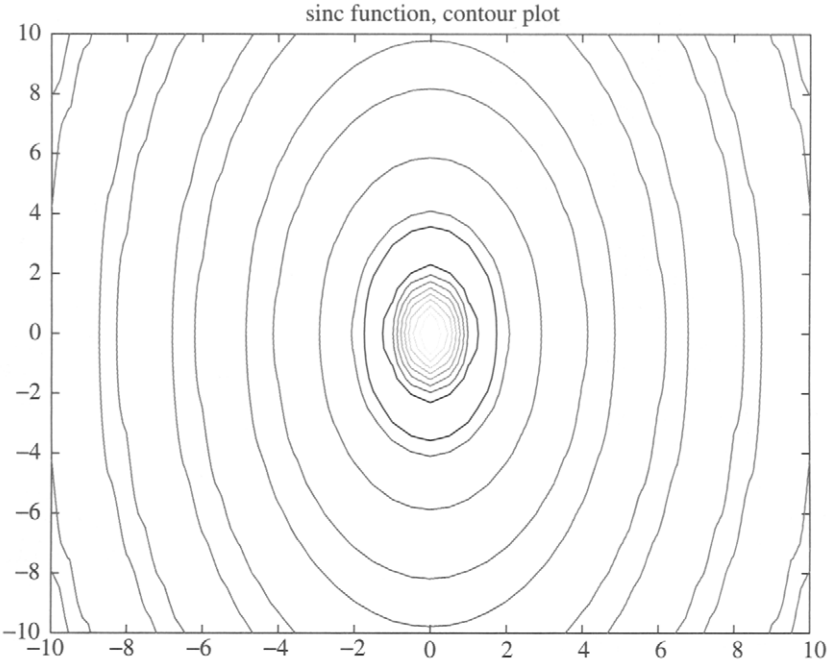

FIGURE 2 Contour plot.

Contour plots are analogous to the contour or topographic maps used to describe geographical locations. The sinc function is shown using this method in Fig. 2. All points which have a specific value are connected to form a continuous line. For a continuous function the lines must form closed loops. This type of plot is useful in locating the position of maxima or minima in images or two-dimensional functions. It is used primarily in spectrum analysis and pattern recognition applications. It is difficult to read values from the contour plot and takes some effort to determine whether the functional trend is up or down. The filled contour plot, available in MATLAB, helps in this last task.

Most monochrome images are displayed using the gray scale plot where the value of a pixel is represented by it relative lightness. Since in most cases, high values are displayed as light and low values are displayed as dark it is easy to determine functional trends. It is almost impossible to determine exact values. For images, which are nonnegative functions, the display is natural; but for functions, which have negative values, can be quite artificial.

In order to use this type of display with functions, the representation must be scaled to fit in the range of displayable gray levels. This is most often done using a min/max scaling, where the function is linearly mapped such that the minimum value appears as black and the maximum value appears as white. This method was used for the sinc function shown in Fig. 3. For the display of functions, the min/max scaling can be effective to indicate trends in the behavior. Scaling for images is another matter.

Let us consider a monochrome image which has been digitized by some device, e.g., a scanner or camera. Without knowing the physical process of digitization, it is impossible to determine the best way to display the image. The proper display of images requires calibration of both the input and output devices. For now, it is reasonable to give some general rules about the display of monochrome images.

1. For the comparison of a sequences of images, it is *imperative* that all images be displayed using the same

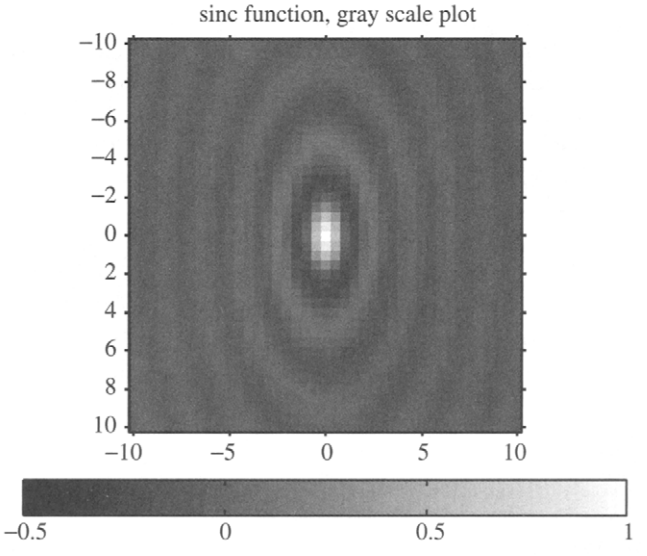

FIGURE 3 Gray scale plot.

scaling. It is hard to emphasize this rule sufficiently and hard to count all the misleading results that have occurred when it has been ignored. The most common violation of this rule occurs when comparing an original and processed image. The user scales both images independently using min/max scaling. In many cases the scaling can produce significant enhancement of low contrast images that can be mistaken for improvements produced by an algorithm under investigation. For example, consider an algorithm designed to reduce noise. The noisy image modelled by

$$\mathbf{g} = \mathbf{f} + \mathbf{n}$$

Since the noise is both positive and negative, the noisy image, **g**, has a larger range than the clean image, **f**. Almost any noise reduction method will reduce the range of the processed image, thus, the output image undergoes additional contrast enhancement if min/max scaling is used. The result is greater apparent dynamic range and a better looking image.

There are several ways to implement this rule. The most appropriate way will depend on the application. The scaling may be done using the min/max of the collection of all images to be compared. In some cases, it is appropriate to truncate values at the limits of the display, rather than force the entire range into the range of the display. This is particularly true of images containing a few outliers. It may be advantageous to reduce the region of the image to a particular region of interest, which will usually reduce the range to be reproduced.

2. Display a step-wedge, a strip of sequential gray levels from minimum to maximum values, with the image to show how the image gray levels are mapped to brightness or density. This allows some idea of the quantitative values associated with the pixels. This is routinely done on images that are used for analysis, such as the digital photographs from space probes.
3. Use a graytone mapping that allows a wide range of gray levels to be visually distinguished. In software such as MATLAB, the user can control the mapping between the continuous values of the image and the values sent to the display device. For example, consider the CRT monitor as the output device. The visual tonal qualities of the output depend on many factors including the brightness and contrast setting of the monitor, the specific phosphors used in the monitor, the linearity of the electron guns and the ambient lighting. It is recommended that adjustments be made so that a user is able to distinguish all levels of a step-wedge of about 32 levels.

Most displays have problems with gray levels at the ends of the range being indistinguishable. This can be overcome by proper adjustment of the contrast and gain controls and an appropriate mapping from image values to display values. For hardcopy devices, the medium should be taken into account. For example, changes in paper type or manufacturer can result in significant tonal variations.

3 Notation and Prerequisite Knowledge

In most cases, the multidimensional process can be represented as a straightforward extension of one-dimensional processes. Thus, it is reasonable to mention the one-dimensional operations that are prerequisite to the chapter and will form the basis of the multidimensional processes.

3.1 Practical Sampling

Mathematically, ideal sampling is usually represented with the use of a *generalized function*, the Dirac delta function, $\delta(t)$ [2]. The entire sampled sequence can be represented using the *comb* function

$$comb(t) = \sum_{n=-\infty}^{\infty} \delta(t - n) \tag{2}$$

where the sampling interval is unity. The sampled signal is obtained by multiplication

$$s_d(t) = s(t)comb(t) = s(t) \sum_{n=-\infty}^{\infty} \delta(t - n) = \sum_{n=-\infty}^{\infty} s(t)\delta(t - n) \tag{3}$$

It is common to use the notation of $\{s(n)\}$ or $s(n)$ to represent the collection of samples in discrete space. The arguments n and t will serve to distinguish the discrete or continuous space.

Practical imaging devices, such as video cameras, CCD arrays and scanners, must use a finite aperture for sampling. The *comb* function cannot be realized by actual devices. The finite aperture is required to obtain a finite amount of energy from the scene. The engineering trade-off is that large apertures receive more light and thus will have higher SNRs than smaller apertures; while smaller apertures have higher spatial resolution than larger ones. This is true for apertures larger than the order of the wavelength of light. At that point diffraction limits the resolution.

The aperture may cause the light intensity to vary over the finite region of integration. For a single sample of a one-dimensional signal at time, nT, the sample value can be obtained by

$$s(n) = \int_{(n-1)T}^{nT} s(t)a(nT - t)dt \tag{4}$$

where $a(t)$ represents the impulse response (or light variation) of the aperture. This is simple convolution. The sampling of the signal can be represented by

$$s(n) = [s(t) * a(t)]comb(t/T) \tag{5}$$

where $*$ represents convolution. This model is reasonably accurate for spatial sampling of most cameras and scanning systems.

The sampling model can be generalized to include the case where each sample is obtained with a different aperture. For this case, the samples, which need not be equally spaced, are given by

$$s(n) = \int_l^u s(t)a_n(t)dt \tag{6}$$

where the limits of integration correspond to the region of support for the aperture. While there may be cases where this form is used in spatial sampling, its main use is in sampling the wavelength dimension of the image signals. That topic will be covered later. The generalized signal reconstruction equation has the form

$$s(t) = \sum_{n=-\infty}^{\infty} s(n)g_n(t) \tag{7}$$

where the collection of functions, $\{g_n(t)\}$, provide the interpolation from discrete to continuous space. The exact form of $\{g_n(t)\}$ depends on the form of $\{a_n(t)\}$.

3.2 One-Dimensional Discrete System Representation

Linear operations on signals and images can be represented as simple matrix multiplications. The internal form of the matrix may be complicated, but the conceptual manipulation of images is very easy. Let us consider the representation of a one-dimensional convolution before going on to multidimensions. Consider the linear, time-invariant system

$$g(t) = \int_{-\infty}^{\infty} h(u)s(t-u)du$$

the discrete approximation to continuous convolution is given by

$$g(n) = \sum_{k=0}^{L-1} h(k)s(n-k) \tag{8}$$

where the indices n and k represent sampling of the analog signals, e.g., $s(n) = s(n\Delta T)$. Since it is assumed that the signals under investigation have finite support, the summation is over a finite number of terms. If $s(n)$ has M nonzero samples and $h(n)$ has L nonzero samples, then $g(n)$ can have at most $N = M + L - 1$ nonzero samples. It is assumed the reader is familiar with what conditions are necessary so that can we represent the analog system by discrete approximation. Using the definition of the signal as a vector, $\mathbf{s} = [s(0), s(1), \ldots s(M-1)]$, the summation of Eq. (8) can be written

$$\mathbf{g} = \mathbf{H}\mathbf{s} \tag{9}$$

where the vectors $\mathbf{s}$ and $\mathbf{g}$ are of length M and N, respectively and the N×M matrix $\mathbf{H}$ is defined by

$$\mathbf{H} = \begin{bmatrix} h_0 & 0 & 0 & \ldots & 0 & 0 & 0 \\ h_1 & h_0 & 0 & \ldots & 0 & 0 & 0 \\ h_2 & h_1 & h_0 & \ldots & 0 & 0 & 0 \\ \vdots & \vdots & \vdots & \vdots & \vdots & \vdots & \vdots \\ h_{L-1} & h_{L-2} & h_{L-3} & \ldots & 0 & 0 & 0 \\ 0 & h_{L-1} & h_{L-2} & \ldots & 0 & 0 & 0 \\ \vdots & \vdots & \vdots & \vdots & \vdots & \vdots & \vdots \\ 0 & 0 & 0 & \ldots & h_0 & 0 & 0 \\ 0 & 0 & 0 & \ldots & h_1 & h_0 & 0 \\ 0 & 0 & 0 & \ldots & h_2 & h_1 & h_0 \\ 0 & 0 & 0 & \ldots & h_3 & h_2 & h_1 \\ \vdots & \vdots & \vdots & \vdots & \vdots & \vdots & \vdots \\ 0 & 0 & 0 & \ldots & 0 & h_{L-1} & h_{L-2} \\ 0 & 0 & 0 & \ldots & 0 & 0 & h_{L-1} \end{bmatrix}$$

It is often desirable to work with square matrices. In this case, the input vector can be padded with zeros to the same size as $\mathbf{g}$ and the matrix $\mathbf{H}$ modified to produce an N×N Toeplitz form

$$\mathbf{H}_t = \begin{bmatrix} h_0 & 0 & 0 & \ldots & 0 & 0 & 0 & \ldots & 0 & 0 & 0 \\ h_1 & h_0 & 0 & \ldots & 0 & 0 & 0 & \ldots & 0 & 0 & 0 \\ h_2 & h_1 & h_0 & \ldots & 0 & 0 & 0 & \ldots & 0 & 0 & 0 \\ \vdots & \vdots & \vdots & \vdots & \vdots & \vdots & \vdots & \vdots & \vdots & \vdots & \vdots \\ h_{L-1} & h_{L-2} & h_{L-3} & \ldots & h_0 & 0 & 0 & \ldots & 0 & 0 & 0 \\ 0 & h_{L-1} & h_{L-2} & \ldots & h_1 & h_0 & 0 & \ldots & 0 & 0 & 0 \\ \vdots & \vdots & \vdots & \vdots & \vdots & \vdots & \vdots & \vdots & \vdots & \vdots & \vdots \\ 0 & 0 & 0 & \ldots & h_k & h_{k-1} & h_{k-2} & \ldots & 0 & 0 & 0 \\ 0 & 0 & 0 & \ldots & h_{k+1} & h_k & h_{k-1} & \ldots & 0 & 0 & 0 \\ 0 & 0 & 0 & \ldots & h_{k+2} & h_{k+1} & h_k & \ldots & 0 & 0 & 0 \\ \vdots & \vdots & \vdots & \vdots & \vdots & \vdots & \vdots & \vdots & \vdots & \vdots & \vdots \\ 0 & 0 & 0 & \ldots & 0 & h_{L-1} & h_{L-2} & \ldots & h_1 & h_0 & 0 \\ 0 & 0 & 0 & \ldots & 0 & 0 & h_{L-1} & \ldots & h_2 & h_1 & h_0 \end{bmatrix}$$

The output can now be written

$$\mathbf{g} = \mathbf{H}_t\mathbf{s}_0$$

where $\mathbf{s}_0 = [s(0), s(1), \ldots s(M-1), 0, \ldots 0]^T$.

It is often useful, because of the efficiency of the FFT, to approximate the Toeplitz form by a circulant form

$$\mathbf{H}_c = \begin{bmatrix} h_0 & 0 & 0 & \dots & 0 & h_{L-1} & h_{L-2} & \dots & h_3 & h_2 & h_1 \\ h_1 & h_0 & 0 & \dots & 0 & 0 & 0 & \dots & h_4 & h_3 & h_2 \\ h_2 & h_1 & h_0 & \dots & 0 & 0 & 0 & \dots & h_5 & h_4 & h_3 \\ \vdots & \vdots & \vdots & \vdots & \vdots & \vdots & \vdots & \vdots & \vdots & \vdots & \vdots \\ h_{L-1} & h_{L-2} & h_{L-3} & \dots & 0 & 0 & 0 & \dots & 0 & 0 & 0 \\ 0 & h_{L-1} & h_{L-2} & \dots & 0 & 0 & 0 & \dots & 0 & 0 & 0 \\ \vdots & \vdots & \vdots & \vdots & \vdots & \vdots & \vdots & \vdots & \vdots & \vdots & \vdots \\ 0 & 0 & 0 & \dots & h_k & h_{k-1} & h_{k-2} & \dots & 0 & 0 & 0 \\ 0 & 0 & 0 & \dots & h_{k+1} & h_k & h_{k-1} & \dots & 0 & 0 & 0 \\ 0 & 0 & 0 & \dots & h_{k+2} & h_{k+1} & h_k & \dots & 0 & 0 & 0 \\ \vdots & \vdots & \vdots & \vdots & \vdots & \vdots & \vdots & \vdots & \vdots & \vdots & \vdots \\ 0 & 0 & 0 & \dots & 0 & h_{L-1} & h_{L-2} & \dots & h_1 & h_0 & 0 \\ 0 & 0 & 0 & \dots & 0 & 0 & h_{L-1} & \dots & h_2 & h_1 & h_0 \end{bmatrix}$$

The approximation of a Toeplitz matrix by a circulant gets better as the dimension of the matrix increases. Consider the matrix norm

$$||\mathbf{H}||^2 = \frac{1}{N^2} \sum_{k=1}^{N} \sum_{l=1}^{N} h_{kl}^2$$

then $||\mathbf{H}_t - \mathbf{H}_c|| \to 0$ as $N \to \infty$. This approximation works well with impulse responses of short duration and autocorrelation matrices with small correlation distances.

3.3 Multidimensional System Representation

The images of interest are described by two spatial coordinates and a wavelength coordinate, $f(x, y, \lambda)$. This continuous image will be sampled in each dimension. The result is a function defined on a discrete coordinate system, $f(m, n, l)$. This would usually require a three-dimensional matrix. However, to allow the use of standard matrix algebra, it is common to use stacked notation [9]. Each band, defined by wavelength λ_l or simply l, of the image is a $P \times P$ image. Without loss of generality, we will use assume a square image for notational simplicity. This image can be represented as a $P^2 \times 1$ vector. The Q bands of the image can be stacked in a like manner forming a $QP^2 \times 1$ vector.

Optical blurring is modeled as convolution of the spatial image. Each wavelength of the image may be blurred by a slightly different point spread function (PSF). This is represented by

$$\mathbf{g}_{(QP^2 \times 1)} = \mathbf{H}_{(QP^2 \times QP^2)} \mathbf{f}_{(QP^2 \times 1)} \tag{10}$$

where the matrix $\mathbf{H}$ has a block form

$$\mathbf{H} = \begin{bmatrix} \mathbf{H}_{1,1} & \mathbf{H}_{1,2} & \dots & \mathbf{H}_{1,Q} \\ \mathbf{H}_{2,1} & \mathbf{H}_{2,2} & \dots & \mathbf{H}_{2,Q} \\ \vdots & \vdots & & \vdots \\ \mathbf{H}_{Q,1} & \mathbf{H}_{Q,2} & \dots & \mathbf{H}_{Q,Q} \end{bmatrix}. \tag{11}$$

The submatrix $\mathbf{H}_{i,j}$ is of dimension $P^2 \times P^2$ and represents the contribution of the jth band of the input to the ith band of the output. Since an optical system does not modify the frequency of an optical signal, $\mathbf{H}$ will be block diagonal. There are cases, e.g., imaging using color filter arrays, where the diagonal assumption does not hold. In many cases, multidimensional processing is a straightforward extension of one-dimensional processing. The use of matrix notation permits the use of simple linear algebra to derive many results that are valid in any dimension. Problems arise primarily during the implementation of the algorithms when simplifying assumptions are usually made. Some of the similarities and differences of 1D and 2D system are listed below.

Similarities:

1. Derivatives and Taylor expansions are extensions of 1D.
2. Fourier transforms are straightforward extension of 1D.
3. Linear systems theory is the same.
4. Sampling theory is straightforward extension of 1D.
5. Separable 2D signals are treated as 1D signals.

Differences:

1. Continuity and derivatives have directional definitions.
2. 2D signals are usually not causal; causality is not intuitive.
3. 2D polynomials cannot always be factored; this limits use of rational polynomial models.
4. More variation in 2D sampling, hexagonal lattices are common in nature, random sampling makes interpolation much more difficult.
5. Periodic functions may have a wide variety of 2D periods.
6. 2D Regions of support are more variable, the boundaries of objects are often irregular instead of rectangular or elliptical.
7. 2D systems can be mixed IIR and FIR, causal and noncausal.
8 Algebraic representation using stacked notation for 2D signals is more difficult to manipulate and understand.

Algebraic representation using stacked notation for 2D signals is more difficult to manipulate and understand than in

1D. An example of this is illustrated by considering the autocorrelation of multiband images which are used in multispectral restoration methods. This is easily written in terms of the matrix notation reviewed earlier:

$$\mathbf{R}_{ff} = E\{\mathbf{f}\mathbf{f}^T\}$$

where $\mathbf{f}$ is a $QP^2 \times 1$ vector. In order to compute estimates, we must be able to manipulate this matrix. While the $QP^2 \times QP^2$ matrix is easily manipulated symbolically, direct computation with the matrix is not practical for realistic values of P and Q, e.g., $Q = 3$, $P = 256$. For practical computation, the matrix form is simplified by using various assumptions, such as separability, circularity and independence of bands. These assumptions result in block properties of the matrix that reduces the dimension of the computation. A good example is shown in the multidimensional restoration problem [33].

4 Analog Images as Physical Functions

The image which exists in the analog world is a spatio-temporal distribution of radiant energy. As was mentioned earlier, this chapter will not discuss the temporal dimension but concentrate on the spatial and wavelength aspects of the image. The function is represented by $f(x, y, \lambda)$. While it is often overlooked by students eager to process their first image, it is fundamental to define what the value of the function represents. Since we are dealing with radiant energy, the value of the function represents energy flux, exactly like electromagnetic theory. The units will be energy per unit area (or angle) per unit time per unit wavelength. From the imaging point of view, the function is described by the spatial energy distribution at the sensor. It does not matter whether the object in the image emits light or reflects light.

To obtain a sample of the analog image, we must integrate over space, time and wavelength to obtain a finite amount of energy. Since we have eliminated time from the description, we can have watts per unit area per unit wavelength. To obtain overall lightness, the wavelength dimension is integrated out using the luminous efficiency function discussed in the following section on colorimetry. The common units of light intensity are lux ($lumens/m^2$) or footcandles. See [17] for an exact definition of radiometric quantities. A table of typical light levels is given in Table 1. The most common instrument for measuring light intensity is the light meter used in professional and amateur photography.

In order to sample an image correctly, we must be able to characterize its energy distribution in each of the dimensions. There is little that can be said about the spatial distribution of energy. From experience, we know that images vary greatly in spatial content. Objects in an image usually may appear at any spatial location and at any orientation. This implies that there is no reason to apply varying sample spacing over the spatial range of an image. In the cases of some very restricted ensembles of images, variable spatial sampling has been used to advantage. Since these examples are quite rare, they will not be discussed here.

TABLE 1 Qualitative description of luminance levels

Description	Lux (Cd/m^2)	Footcandles
Moonless night	$\sim 10^{-6}$	$\sim 10^{-7}$
Full moon night	$\sim 10^{-3}$	$\sim 10^{-4}$
Restaurant	~ 100	~ 9
Office	~ 350	~ 33
Overcast day	~ 5000	~ 465
Sunny day	$\sim 200{,}000$	~ 18600

Spatial sampling is done using a regular grid. The grid is most often rectilinear but hexagonal sampling has been thoroughly investigated [3]. Hexagonal sampling is used for efficiency when the images have a natural circular region of support or circular symmetry. All the mathematic operations, such as Fourier transforms and convolutions, exist for hexagonal grids. It is noted that the reasons for uniform sampling of the temporal dimension follow the same arguments.

The distribution of energy in the wavelength dimension is not as straightforward to characterize. In addition, we are often not interested in reconstructing the radiant spectral distribution as we are the spatial distribution. We are interested in constructing an image that appears to the human to be the same colors as the original image. In this sense, we are actually using color aliasing to our advantage. Because of this aspect of color imaging, we need to characterize the color vision system of the eye in order to determine proper sampling of the wavelength dimension.

5 Colorimetry

To understand the fundamental difference in the wavelength-domain, it is necessary to describe some of the fundamentals of color vision and color measurement. What is presented here is only a brief description that will allow us to preceed with the description of the sampling and mathematic representation of color images. A more complete description of the human color visual system can be found in [4, 5].

The retina contains two types of light sensors, rods, and cones. The rods are used for monochrome vision at low light levels; the cones are used for color vision at higher light levels. There are three types of cones. Each type is maximally sensitive to a different part of the spectrum. They are often referred to as long, medium and short wavelength regions. A common description refers to them as red, green, and blue cones, although their maximal sensitivity is in the yellow,

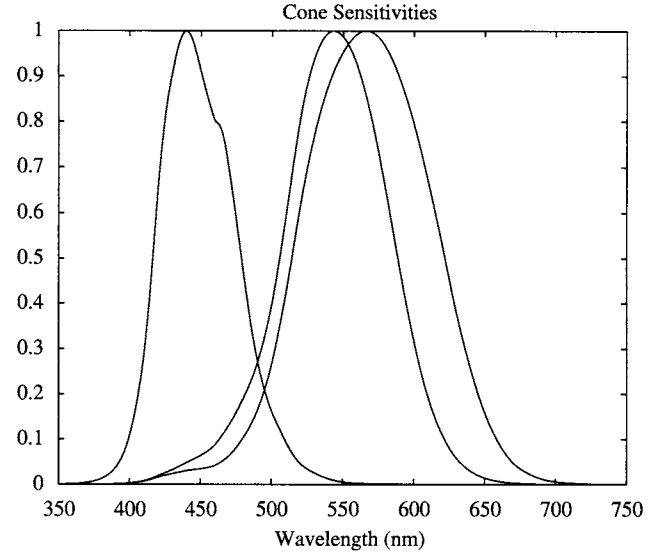

FIGURE 4 Cone sensitivities.

green, and blue regions of the spectrum. Recall that the visible spectrum extends from about 400 nm (blue) to about 700 nm (red). Cones sensitivities are related to the absorption sensitivity of the pigments in the cones. The absorption sensitivity of the different cones has been measured by several workers. An example of the curves is shown in Fig. 4. Long before the technology was available to measure the curves directly, they were estimated from a clever color matching experiment. A description of this experiment, which is still used today can be found in [15, 17].

Grassmann formulated a set of laws for additive color mixture in 1853 [6, 7, 17]. Additive in this sense refers to the addition of two or more radiant sources of light. In addition, Grassmann conjectured that any additive color mixture could be matched by the proper amounts of three primary stimuli. Considering what was known about the physiology of the eye at that time, these laws represent considerable insight. It should be noted that these "laws" are not physically exact but represent a good approximation under a wide range of visibility conditions. There is current research in the vision and color science community on the refinements and reformulations of the laws.

Grassmann's laws are essentially unchanged as printed in recent texts on color science [17]. With our current understanding of the physiology of the eye and a basic background in linear algebra, Grassmann's laws can be stated more concisely. Furthermore, extensions of the laws and additional properties are easily derived using the mathematics of matrix theory. There have been several papers which have taken a linear systems approach to describing color spaces as defined by a standard human observer, [5, 8, 12, 14]. This section will briefly summarize these results and relate them to simple signal processing concepts. For the purposes of this work, it is sufficient to note that the spectral responses of the three types of sensors are sufficiently different so as to define a three-dimensional vector space.

5.1 Color Sampling

The mathematic model for the color sensor of a camera or the human eye can be represented by

$$v_k = \int_{-\infty}^{\infty} r_a(\lambda) m_k(\lambda) d\lambda, \; k = 1, 2, 3 \tag{12}$$

where $r_a(\lambda)$ is the radiant distribution of light as a function of wavelength and $m_k(\lambda)$ is the sensitivity of the kth color sensor. The sensitivity functions of the eye were shown in Fig. 4.

Note that sampling of the radiant power signal associated with a color image can be viewed in at least two ways. If the goal of the sampling is to reproduce the spectral distribution, then the same criteria for sampling the usual electronic signals can be directly applied. However, the goal of color sampling is not often to reproduce the spectral distribution but to allow reproduction of the color sensation. This aspect of color sampling will be discussed in detail below. To keep this discussion as simple as possible, we will treat the color sampling problem as a subsampling of a high resolution discrete space, that is, the N samples are sufficient to reconstruct the original spectrum using the uniform sampling of Section 3.

It has been assumed in most research and standards work that the visual frequency spectrum can be sampled finely enough to allow the accurate use of numeric approximation of integration. A common sample spacing is 10 nanometers over the range 400–700 nm, although ranges as wide as 360–780 nm have been used. This is used for many color tables and lower priced instrumentation. Precision color instrumentation produces data at 2 nm intervals. Finer sampling is required for some illuminants with line emitters. Reflective surfaces are usually smoothly varying and can be accurately sampled more coarsely. Sampling of color signals is discussed in Section 6 and in detail in [10].

Proper sampling follows the same bandwidth restrictions that govern all digital signal processing. Following the assumption that the spectrum can be adequately sampled, the space of all possible visible spectra lies in an N-dimensional vector space, where $N = 31$ is the range if 400–700 nm is used. The spectral response of each of the eye's sensors can be sampled as well, giving three linearly independent N-vectors which define the visual subspace.

Under the assumption of proper sampling, the integral of Eq. (12) can be well approximated by a summation

$$v_k = \sum_{n=L}^{U} r_a(n\Delta\lambda) s_k(n\Delta\lambda) \tag{13}$$

where $\Delta\lambda$ represents the sampling interval and the summation limits are determined by the region of support of the sensitivity of the eye. The above equations can be generalized to represent any color sensor by replacing $s_k(\cdot)$ with $m_k(\cdot)$. This discrete form is easily represented in matrix/vector notation. This will be done in the following sections.

5.2 Discrete Representation of Color Matching

The response of the eye can be represented by a matrix, $\mathbf{S} = [\mathbf{s}_1, \mathbf{s}_2, \mathbf{s}_3]$, where the N-vectors, $\mathbf{s}_i$, represent the response of the i^{th} type sensor (cone). Any visible spectrum can be represented by an N-vector, $\mathbf{f}$. The response of the sensors to the input spectrum is a 3-vector, $\mathbf{t}$, obtained by

$$\mathbf{t} = \mathbf{S}^T\mathbf{f} \tag{14}$$

Two visible spectra are said to have the same color if they appear the same to the human observer. In our linear model, this means that if $\mathbf{f}$ and $\mathbf{g}$ are two N-vectors representing different spectral distributions, they are equivalent colors if

$$\mathbf{S}^T\mathbf{f} = \mathbf{S}^T\mathbf{g} \tag{15}$$

It is clear that there may be many different spectra that appear to be the same color to the observer. Two spectra that appear the same are called metamers. Metamerism (meh tam er ism) is one of the greatest and most fascinating problems in color science. It is basically color "aliasing" and can be described by the generalized sampling described earlier.

It is difficult to find the matrix, $\mathbf{S}$, that defines the response of the eye. However, there is a conceptually simple experiment that is used to define the human visual space defined by $\mathbf{S}$. A detailed discussion of this experiment is given in [15, 17]. Consider the set of monochromatic spectra $\mathbf{e}_i$, for $i = 1, 2, ...N$. The N-vectors, $\mathbf{e}_i$, have a one in the ith position and zeros elsewhere. The goal of the experiment is to match each of the monochromatic spectra with a linear combination of primary spectra. Construct three lighting sources that are linearly independent in N-space. Let the matrix, $\mathbf{P} = [\mathbf{p}_1, \mathbf{p}_2, \mathbf{p}_3]$, represent the spectral content of these primaries. The phosphors of a color television are a common example, Fig. 5.

An experiment is conducted where a subject is shown one of the monochromactic spectra, $\mathbf{e}_i$, on one half of a visual field. On the other half of the visual field appears a linear combination of the primary sources. The subject attempts to visually match an input monochromatic spectrum by adjusting the relative intensities of the primary sources. Physically, it may be impossible to match the input spectrum by adjusting the intensities of the primaries. When this happens, the subject is allowed to change the field of one of the primaries so that it

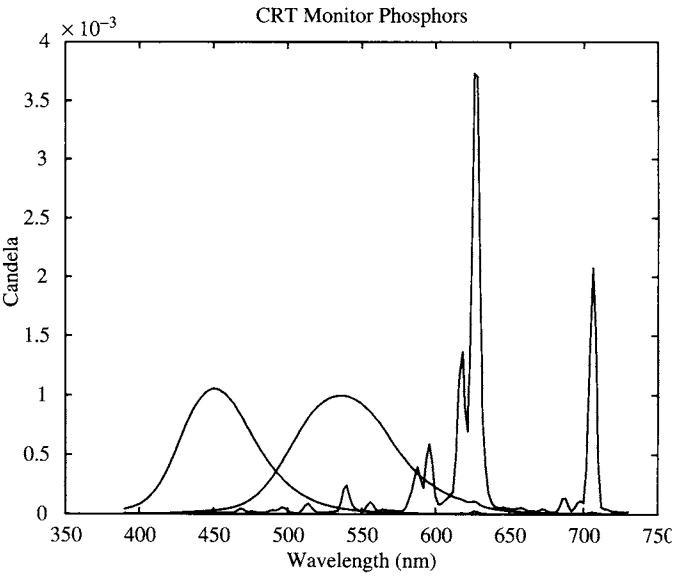

FIGURE 5 CRT monitor phosphors.

falls on the same field as the monochromatic spectrum. This is mathematically equivalent to subtracting that amount of primary from the primary field. Denoting the relative intensities of the primaries by the three-vector $\mathbf{a}_i = [a_{i1}, a_{i2}, a_{i3}]^T$, the match is written mathematically as

$$\mathbf{S}^T\mathbf{e}_i = \mathbf{S}^T\mathbf{P}\mathbf{a}_i \tag{16}$$

Combining the results of all N monochromatic spectra, Eq. (5) can be written

$$\mathbf{S}^T\mathbf{I} = \mathbf{S}^T = \mathbf{S}^T\mathbf{P}\mathbf{A}^T \tag{17}$$

where $\mathbf{I} = [\mathbf{e}_1, \mathbf{e}_2, ..., \mathbf{e}_N]$ is the NxN identity matrix.

Note that because the primaries, $\mathbf{P}$, are not metameric, the product matrix is nonsingular, i.e., $(\mathbf{S}^T\mathbf{P})^{-1}$ exists. The Human Visual Subspace (HVSS) in the N-dimensional vector space is defined by the column vectors of $\mathbf{S}$; however, this space can be equally well defined by any nonsingular transformation of those basis vectors. The matrix,

$$\mathbf{A} = \mathbf{S}(\mathbf{P}^T\mathbf{S})^{-1} \tag{18}$$

is one such transformation. The columns of the matrix $\mathbf{A}$ are called the color matching functions associated with the primaries $\mathbf{P}$.

To avoid the problem of negative values, which cannot be realized with transmission or reflective filters, the CIE developed a standard transformation of the color matching functions, which have no negative values. This set of color matching functions is known as the *standard observer* or the CIE XYZ color matching functions. These functions are shown

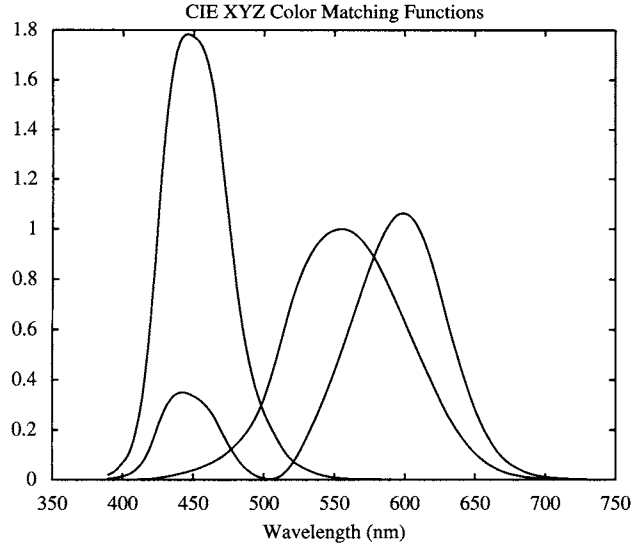

FIGURE 6 CIE XYZ color matching functions.

in Fig. 6. For the remainder of this chapter, the matrix, $\mathbf{A}$, can be thought of as this standard set of functions.

5.3 Properties of Color Matching Functions

Having defined the human visual subspace, it is worthwhile examining some of the common properties of this space. Because of the relatively simple mathematic definition of color matching given in the last section, the standard properties enumerated by Grassmann are easily derived by simple matrix manipulations [12]. These properties play an important part in color sampling and display.

Property 1 (Dependence of Color on A)

Two visual spectra, $\mathbf{f}$ and $\mathbf{g}$, appear the same if and only if $\mathbf{A}^T\mathbf{f} = \mathbf{A}^T\mathbf{g}$. Writing this mathematically, $\mathbf{S}^T\mathbf{f} = \mathbf{S}^T\mathbf{g}$ if $\mathbf{A}^T\mathbf{f} = \mathbf{A}^T\mathbf{g}$. Metamerism is color aliasing. Two signals $\mathbf{f}$ and $\mathbf{g}$ are sampled by the cones or equivalently by the color matching functions and produce the same tristimulus values.

The importance of this property is that any linear transformation of the sensitivities of the eye or the CIE color matching functions can be used to determine a color match. This gives more latitude in choosing color filters for cameras and scanners, as well as for color measurement equipment. It is this property that is the basis for the design of optimal color scanning filters [13, 30].

A note on terminology is appropriate here. When the color matching matrix is the CIE standard [17], the elements of the 3-vector defined by $\mathbf{t} = \mathbf{A}^T\mathbf{f}$ are called tristimulus values and usually denoted by X, Y, Z; i.e., $\mathbf{t}^T = [X, Y, Z]$. The chromaticity of a spectrum is obtained by normalizing the tristimulus values,

$$x = X/(X + Y + Z)$$

$$y = Y/(X + Y + Z)$$

$$z = Z/(X + Y + Z)$$

Since the chromaticity coordinates have been normalized, any two of them are sufficient to characterize the chromaticity of a spectrum. The x and y terms are the standard for describing chromaticity. It is noted that the convention of using different variables for the elements of the tristimulus vector may make mental conversion between the vector space notation and notation in common color science texts more difficult.

The CIE has chosen the $\mathbf{a}_2$ sensitivity vector to correspond to the luminance efficiency function of the eye. This function, shown as the middle curve in Fig. 6, gives the relative sensitivity of the eye to the energy at each wavelength. The Y tristimulus value is called luminance and indicates the perceived brightness of a radiant spectrum. It is this value that is used to calculate the effective light output of light bulbs in lumens. The chromaticities x and y indicate the hue and saturation of the color. Often the color is described in terms of $[x, y, Y]$ because of the ease of interpretation. Other color coordinate systems will be discussed later.

Property 2 (Transformation of Primaries)

If a different set of primary sources, $\mathbf{Q}$, are used in the color matching experiment, a different set of color matching functions, $\mathbf{B}$, are obtained. The relation between the two color matching matrices is given by

$$\mathbf{B}^T = (\mathbf{A}^T\mathbf{Q})^{-1}\mathbf{A}^T \tag{19}$$

The more common interpretation of the matrix $\mathbf{A}^T\mathbf{Q}$ is obtained by a direct examination. The jth column of $\mathbf{Q}$, denoted $\mathbf{q}_j$, is the spectral distribution of the jth primary of the new set. The element $[\mathbf{A}^T\mathbf{Q}]_{i,j}$ is the amount of the primary $\mathbf{p}_i$ required to match primary $\mathbf{q}_j$. It is noted that the above form of the change of primaries is restricted to those that can be adequately represented under the assumed sampling discussed previously. In the case that one of the new primaries is a Dirac delta function located between sample frequencies, the transformation $\mathbf{A}^T\mathbf{Q}$ must be found by interpolation. The CIE RGB color matching functions are defined by the monochromatic lines at 700 nm, 546.1 nm, and 435.8 nm, shown in Fig. 7. The negative portions of these functions are particularly important since it implies that all color matching functions associated with realizable primaries have negative portions.

One of the uses of this property is in determining the filters for color television cameras. The color matching functions associated with the primaries used in a television monitor are the ideal filters. The tristimulus values obtained by such filters would directly give the values to drive the color guns. The NTSC standard $[R, G, B]$ are related to these color matching functions. For coding purposes and efficient use of

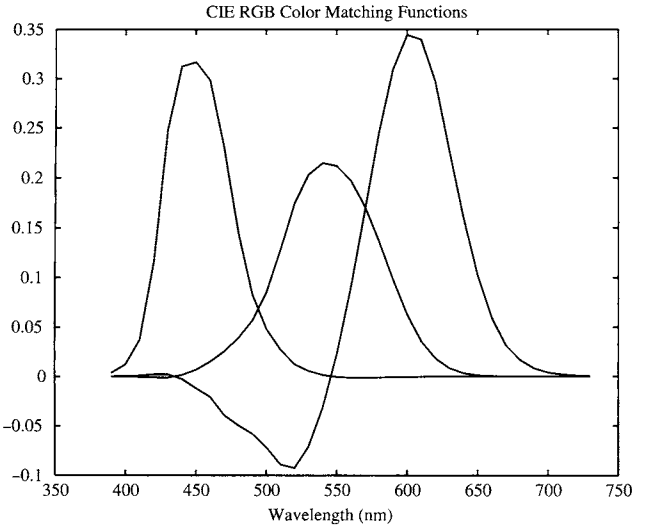

FIGURE 7 CIE XYZ color matching functions.

band-width, the RGB values are transformed to YIQ values, where Y is the CIE Y (luminance) and, I and Q carry the hue and saturation information. The transformation is a 3×3 matrix multiplication [9] (see property 3 below).

Unfortunately, since the TV primaries are realizable, the color matching functions that correspond to them are not. This means that the filters which are used in TV cameras are only an approximation to the ideal filters. These filters are usually obtained by simply clipping the part of the ideal filter which falls below zero. This introduces an error which cannot be corrected by any postprocessing.

Property 3 (Transformation of Color Vectors)

If $\mathbf{c}$ and $\mathbf{d}$ are the color vectors in 3-space associated with the visible spectrum, $\mathbf{f}$, under the primaries $\mathbf{P}$ and $\mathbf{Q}$ respectively, then

$$\mathbf{d} = (\mathbf{A}^T\mathbf{Q})^{-1}\mathbf{c} \tag{20}$$

where $\mathbf{A}$ is the color matching function matrix associated with primaries $\mathbf{P}$. This states that a 3×3 transformation is all that is required to go from one color space to another.

Property 4 (Metamers and the Human Visual Subspace)

The N dimensional spectral space can be decomposed into a 3-dimensional subspace known as the Human Visual Subspace (HVSS) and an N 3-dimensional subspace known as the black space. All metamers of a particular visible spectrum, $\mathbf{f}$, are given by

$$\mathbf{x} = \mathbf{P}_v\mathbf{f} + \mathbf{P}_b\mathbf{g} \tag{21}$$

where $\mathbf{P}_v = \mathbf{A}(\mathbf{A}^T\mathbf{A})^{-1}\mathbf{A}^T$ is the orthogonal projection operator to the visual space, $\mathbf{P}_b = [\mathbf{I} - \mathbf{A}(\mathbf{A}^T\mathbf{A})^{-1}\mathbf{A}^T]$ is the orthogonal projection operator to the black space, and $\mathbf{g}$ is any vector in N-space.

It should be noted that humans cannot see (or detect) all possible spectra in the visual space. Since it is a vector space, there exist elements with negative values. These elements are not realizable and thus cannot be seen. All vectors in the black space have negative elements. While the vectors in the black space are not realizable and cannot be seen, they can be combined with vectors in the visible space to produce a realizable spectrum.

Property 5 (Effect of Illumination)

The effect of an illumination spectrum, represented by the N-vector $\mathbf{l}$, is to transform the color matching matrix $\mathbf{A}$ by

$$\mathbf{A}_l = \mathbf{L}\mathbf{A} \tag{22}$$

where $\mathbf{L}$ is a diagonal matrix defined by setting the diagonal elements of $\mathbf{L}$ to the elements of the vector $\mathbf{l}$. The emitted spectrum for an object with reflectance vector, $\mathbf{r}$, underillumination, $\mathbf{l}$, is given by multiplying the reflectance by the illuminant at each wavelength, $\mathbf{g} = \mathbf{L}\mathbf{r}$. The tristimulus values associated with this emitted spectrum is obtained by

$$\mathbf{t} = \mathbf{A}^T\mathbf{g} = \mathbf{A}^T\mathbf{L}\mathbf{r} = \mathbf{A}_l^T\mathbf{r} \tag{23}$$

The matrix $\mathbf{A}_l$ will be called the color matching functions under illuminant $\mathbf{l}$.

Metamerism under different illuminants is one of the greatest problems in color science. A common imaging example occurs in making a digital copy of an original color image, e.g., a color copier. The user will compare the copy to the original under the light in the vicinity of the copier. The copier might be tuned to produce good matches under the fluorescent lights of a typical office but may produce copies that no longer match the original when viewed under the incandescent lights of another office or viewed near a window that allows a strong daylight component.

A typical mismatch can be expressed mathematically by relations

$$\mathbf{A}^T\mathbf{L}_f\mathbf{r}_1 = \mathbf{A}^T\mathbf{L}_f\mathbf{r}_2 \tag{24}$$

$$\mathbf{A}^T\mathbf{L}_d\mathbf{r}_1 \neq \mathbf{A}^T\mathbf{L}_d\mathbf{r}_2 \tag{25}$$

where $\mathbf{L}_f$ and $\mathbf{L}_d$ are diagonal matrices representing standard fluorescent and daylight spectra respectively, and $\mathbf{r}_1$ and $\mathbf{r}_2$ represent the reflectance spectra of the original and copy respectively. The ideal images would have $\mathbf{r}_2$ matching $\mathbf{r}_1$ under all illuminations, which would imply they are equal. This is virtually impossible since the two images are made with different colorants.

If the appearance of the image under a particular illuminant is to be recorded, then the scanner must have sensitivities that are within a linear transformation of the color matching functions under that illuminant. In this case, the scanner consists of an illumination source, a set of filters and a detector. The product of the three must duplicate the desired color matching functions.

$$\mathbf{A}_l = \mathbf{LA} = \mathbf{L}_s\mathbf{DM} \tag{26}$$

where $\mathbf{L}_s$ is a diagonal matrix defined the scanner illuminant, $\mathbf{D}$ is the diagonal matrix defined by the spectral sensitivity of the detector and $\mathbf{M}$ is the N×3 matrix defined by the transmission characteristics of the scanning filters. In some modern scanners, three colored lamps are used instead of a single lamp and three filters. In this case, the $\mathbf{L}_s$ and $\mathbf{M}$ matrices can be combined.

In most applications the scanner illumination is a high intensity source, so as to minimize scanning time. The detector is usually a standard CCD array or photomultiplier tube. The design problem is to create a filter set $\mathbf{M}$ which brings the product in Eq. (26) to within a linear transformation of $\mathbf{A}_l$. Since creating a perfect match with real materials is a problem, it is of interest to measure the goodness of approximations to a set of scanning filters which can be used to design optimal realizable filter sets [13, 30].

5.4 Notes on Sampling for Color Aliasing

Sampling of the radiant power signal associated with a color image can be viewed in at least two ways. If the goal of the sampling is to reproduce the spectral distribution, then the same criteria for sampling the usual electronic signals can be directly applied. However, the goal of color sampling is not often to reproduce the spectral distribution but to allow reproduction of the color sensation. To illustrate this problem, let us consider the case of a television system. The goal is to sample the continuous color spectrum in such a way that the color sensation of the spectrum can be reproduced by the monitor.

A scene is captured with a television camera. We will consider only the color aspects of the signal, i.e., a single pixel. The camera uses three sensors with sensitivities $\mathbf{M}$ to sample the radiant spectrum. The measurements are given by

$$\mathbf{v} = \mathbf{M}^T\mathbf{r} \tag{27}$$

where $\mathbf{r}$ is a high resolution sampled representation of the radiant spectrum and $\mathbf{M} = [\mathbf{m}_1, \mathbf{m}_2, \mathbf{m}_3]$ represent the high resolution sensitivities of the camera. The matrix $\mathbf{M}$ includes the effects of the filters, detectors and optics.

These values are used to reproduce colors at the television receiver. Let us consider the reproduction of color at the receiver by a linear combination of the radiant spectra of the three phosphors on the screen, denoted $\mathbf{P} = [\mathbf{p}_1, \mathbf{p}_2, \mathbf{p}_3]$, where $\mathbf{p}_k$ represent the spectra of the red, green, and blue phosphors. We will also assume that the driving signals, or control values, for the phosphors to be linear combinations of the values measured by the camera, $\mathbf{c} = \mathbf{Bv}$. The reproduced spectrum is $\hat{\mathbf{r}} = \mathbf{Pc}$.

The appearance of the radiant spectra is determined by the response of the human eye

$$\mathbf{t} = \mathbf{S}^T\mathbf{r} \tag{28}$$

where $\mathbf{S}$ is defined by Eq. (14). The tristimulus values of the spectrum reproduced by the TV are obtained by

$$\hat{\mathbf{t}} = \mathbf{S}^T\hat{\mathbf{r}} = \mathbf{S}^T\mathbf{PBM}^T\mathbf{r} \tag{29}$$

If the sampling is done correctly, the tristimulus values can be computed, that is, $\mathbf{B}$ can be chosen so that $\mathbf{t} = \hat{\mathbf{t}}$. Since the three primaries are not metameric and the eye's sensitivities are linearly independent, $(\mathbf{S}^T\mathbf{P})^{-1}$ exists and from the equality we have

$$(\mathbf{S}^T\mathbf{P})^{-1}\mathbf{S}^T = \mathbf{BM}^T \tag{30}$$

since equality of tristimulus values holds for all $\mathbf{r}$. This means that the color spectrum is sampled properly if the sensitivities of the camera are within a linear transformation of the sensitivities of the eye, or equivalently the color matching functions.

Considering the case where the number of sensors, Q, in the camera or any color measuring device is larger than three, the condition is that the sensitivities of the eye must be linear combination of the sampling device sensitivities. In this case,

$$(\mathbf{S}^T\mathbf{P})^{-1}\mathbf{S}^T = \mathbf{B}_{3\times Q}\mathbf{M}^T_{Q\times N} \tag{31}$$

There are still only three types of cones which are described by $\mathbf{S}$. However, the increase in the number of basis functions used in the measuring device allows more freedom to the designer of the instrument. From the vector space viewpoint, the sampling is correct if the three-dimensional vector space defined by the cone sensitivity functions lies within the N-dimensional vector space defined by the device sensitivity functions.

Let us now consider the sampling of reflective spectra. Since color is measured for radiant spectra, a reflective object must be illuminated to be seen. The resulting radiant spectra is the product of the illuminant and the reflection of the object

$$\mathbf{r} = \mathbf{Lr}_0 \tag{32}$$

where $\mathbf{L}$ is diagonal matrix containing the high resolution sampled radiant spectrum of the illuminant and the elements of the reflectance of the object are constrained, $0 \leq \mathbf{r}_0(k) \leq 1$.

To consider the restrictions required for sampling a reflective object, we must account for two illuminants: the illumination under which the object is to be viewed and the illumination under which the measurements are made. The equations for computing the tristimulus values of reflective objects under the viewing illuminant $\mathbf{L}_v$ are given by

$$\mathbf{t} = \mathbf{A}^T\mathbf{L}_v\mathbf{r}_0 \tag{33}$$

where we have used the CIE color matching functions instead of the sensitivities of the eye, (Property 1). The equation for estimating the tristimulus values from the sampled data is given by

$$\hat{\mathbf{t}} = \mathbf{B}\mathbf{M}^T\mathbf{L}_d\mathbf{r}_0 \tag{34}$$

where $\mathbf{L}_d$ is a matrix containing the illuminant spectrum of the device. The sampling is proper if there exists a $\mathbf{B}$ such that

$$\mathbf{B}\mathbf{M}^T\mathbf{L}_d = \mathbf{A}^T\mathbf{L}_v \tag{35}$$

It is noted that in practical applications the device illuminant usually places severe limitations on the problem of approximating the color matching functions under the viewing illuminant. In most applications the scanner illumination is a high intensity source, so as to minimize scanning time. The detector is usually a standard CCD array or photomultiplier tube. The design problem is to create a filter set $\mathbf{M}$ which brings the product of the filters, detectors and optics to within a linear transformation of $\mathbf{A}_l$. Since creating a perfect match with real materials is a problem, it is of interest to measure the goodness of approximations to a set of scanning filters which can be used to design optimal realizable filter sets [13, 30].

5.5 A Note on the Nonlinearity of the Eye

It is noted here that most physical models of the eye include some type of nonlinearity in the sensing process. This nonlinearity is often modelled as a logarithm; in any case, it is always assumed to be monotonic within the intensity range of interest. The nonlinear function, $\mathbf{v} = V(\mathbf{c})$, transforms the 3-vector in an element independent manner; that is,

$$[v_1, v_2, v_3]^T = [V(c_1), V(c_2), V(c_3)]^T \tag{36}$$

Since equality is required for a color match by Eq. (2), the function $V(\cdot)$ does not affect our definition of equivalent colors. Mathematically,

$$V(\mathbf{S}^T\mathbf{f}) = V(\mathbf{S}^T\mathbf{g}) \tag{37}$$

is true if, and only if, $\mathbf{S}^T\mathbf{f} = \mathbf{S}^T\mathbf{g}$. This nonlinearity does have a definite effect on the relative sensitivity in the color matching process and is one of the causes of much searching for the "uniform color space" discussed next.

5.6 Uniform Color Spaces

It has been mentioned that the psychovisual system is known to be nonlinear. The problem of color matching can be treated by linear systems theory, since the receptors behave in a linear mode and exact equality is the goal. In practice, it is seldom that an engineer can produce an exact match to any specification. The nonlinearities of the visual system play a critical role in the determination of a color sensitivity function. Color vision is too complex to be modelled by a simple function. A measure of sensitivity that is consistent with the observations of arbitrary scenes are well beyond present capability. However, much work has been done to determine human color sensitivity in matching two color fields which subtend only a small portion of the visual field.

Some of the first controlled experiments in color sensitivity were done by MacAdam [11]. The observer viewed a disk made of two hemispheres of different colors on a neutral background. One color was fixed; the other could be adjusted by the user. Since MacAdam's pioneering work there have been many additional studies of color sensitivity. Most of these have measured the variability in three dimensions which yields sensitivity ellipsoids in tristimulus space. The work by Wyszecki and Felder [16] is of particular interest as it shows the variation between observers and between a single observer at different times. The large variation of the sizes and orientation of the ellipsoids indicates that mean square error in tristimulus space is a very poor measure of color error. A common method of treating the nonuniform error problem is to transform the space into one where the Euclidean distance is more closely correlated with perceptual error. The CIE recommended two transformations in 1976 in an attempt to standardize measures in the industry.

Neither of the CIE standards exactly achieve the goal of a uniform color space. Given the variability of the data, it is unreasonable to expect that such a space could be found. The transformations do reduce the variations in the sensitivity ellipses by a large degree. They have another major feature in common: the measures are made relative to a reference white point. By using the reference point the transformations attempt to account for the adpative characteristics of the visual system. The CIELab (see-lab) space is

defined by

$$L^* = 116(Y/Y_n)^{1/3} - 16 \tag{38}$$

$$a^* = 500[(X/X_n)^{1/3} - (Y/Y_n)^{1/3}] \tag{39}$$

$$b^* = 200[(Y/Y_n)^{1/3} - (Z/Z_n)^{1/3}] \tag{40}$$

for $X/X_n, Y/Y_n, Z/Z_n > 0.01$. The values X_n, Y_n, Z_n are the tristimulus values of the reference white under the reference illumination, and X, Y, Z are the tristimulus values which are to be mapped to the Lab color space. The restriction that the normalized values be greater than 0.01 is an attempt to account for the fact that at low illumination the cones become less sensitive and the rods (monochrome receptors) become active. A linear model is used at low light levels. The exact form of the linear portion of CIELab and the definition of the CIELuv (see-luv) transformation can be found in [9, 17].

A more recent modification of the CIELab space was created in 1994, called appropriately CIELab94, [34]. This modification addresses some of the short-comings of the 1931 and 1976 versions. However, it is significantly more complex and costly to compute. A major difference is the inclusion of weighting factors in the summation of square errors, instead of using a strict Euclidean distance in the space.

The color error between two colors $\mathbf{c}_1$ and $\mathbf{c}_2$ are measured in terms of

$$\Delta E_{ab} = [(L_1^* - L_2^*)^2 + (a_1^* - a_2^*)^2 + (b_1^* - b_2^*)^2]^{1/2} \tag{41}$$

where $\mathbf{c}_i = [L_i^*, a_i^*, b_i^*]$. A useful rule of thumb is that two colors cannot be distinguished in a scene if their ΔE_{ab} value is less than 3. The ΔE_{ab} threshold is much lower in the experimental setting than in pictorial scenes. It is noted that the sensitivities discussed above are for flat fields. The sensitivity to modulated color is a much more difficult problem.

6 Sampling of Color Signals and Sensors

It has been assumed in most of this chapter that the color signals of interest can be sampled sufficiently well to permit accurate computation using discrete arithmetic. It is appropriate to consider this assumption quantitatively. From the previous sections, it is seen that there are three basic types of color signals to consider: reflectances, illuminants, and sensors. Reflectances usually characterize everyday objects but occasionally man-made items with special properties such as filters and gratings are of interest. Illuminants vary a great deal from natural daylight or moonlight to special lamps used in imaging equipment. The sensors most often used in colorevaluation are those of the human eye. However, because

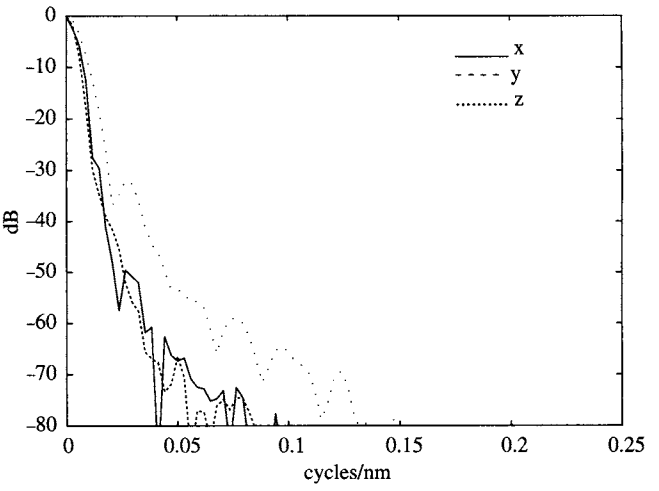

FIGURE 8 Power spectrum of CIE XYZ color matching functions.

of their use in scanners and cameras, CCDs and photomultiplier tubes are of great interest.

The most important sensor characteristics are the cone sensitivities of the eye or equivalently, the color matching functions, e.g., Fig. 6. It is easily seen that functions in Figs. 4, 6 and 7 are very smooth functions and have limited bandwidths. A note on bandwidth is appropriate here. The functions represent continuous functions with finite support. Because of the finite support constraint, they cannot be bandlimited. However, they are clearly smooth and have very low power outside of a very small frequency band. Using 2 nm representations of the functions, the power spectra of these signals are shown in Fig. 8. The spectra represent the Welch estimate where the data is first windowed, then the magnitude of the DFT is computed [2]. It is seen that 10 nm sampling produces very small aliasing error.

In the context of cameras and scanners, the actual photoelectric sensor should be considered. Fortunately, most sensors have very smooth sensitivity curves which have bandwidths comparable to those of the color matching functions. See any handbook of CCD sensors or photomultiplier tubes. Reducing the variety of sensors to be studied can also be justified by the fact that filters can be designed to compensate for the characteristics of the sensor and bring the combination within a linear combination of the CMFs.

The function $r(\lambda)$, which is sampled to give the vector $\mathbf{r}$ used in the colorimetry section, can represent either reflectance or transmission. Desktop scanners usually work with reflective media. There are, however, several film scanners on the market which are used in this type of environment. The larger dynamic range of the photographic media implies a larger bandwidth. Fortunately, there is not a large difference over the range of everyday objects and images. Several ensembles were used for a study in an attempt to include the range of spectra encountered by image scanners

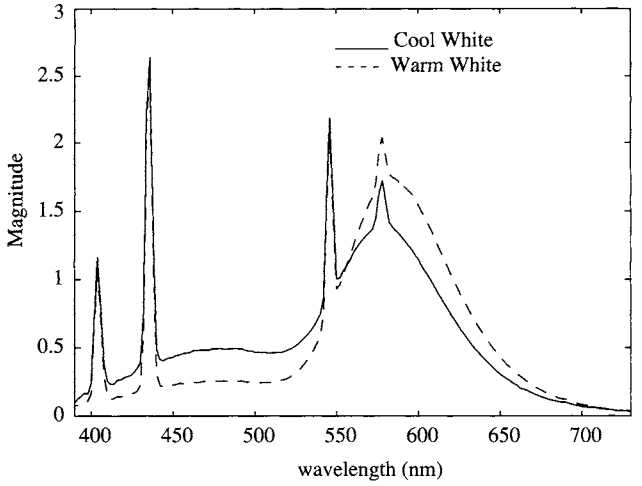

FIGURE 9 Cool white fluorescent and warm white fluorescent.

and color measurement instrumentation [21]. The results showed again that 10 nm sampling was sufficient [10].

There are three major types of viewing illuminants of interest for imaging: daylight, incandescent and fluorescent. There are many more types of illuminants used for scanners and measurement instruments. The properties of the three viewing illuminants can be used as a guideline for sampling and signal processing which involves other types. It has been shown that the illuminant is the determining factor for the choice of sampling interval in the wavelength domain [10].

Incandescent lamps and natural daylight can be modeled as filtered blackbody radiators. The wavelength spectra are relatively smooth and have relatively small bandwidths. As with previous color signals, they are adequately sampled at 10 nm. Office lighting is dominated by fluorescent lamps. Typical wavelength spectra and their frequency power spectra are shown in Figs. 9 and 10.

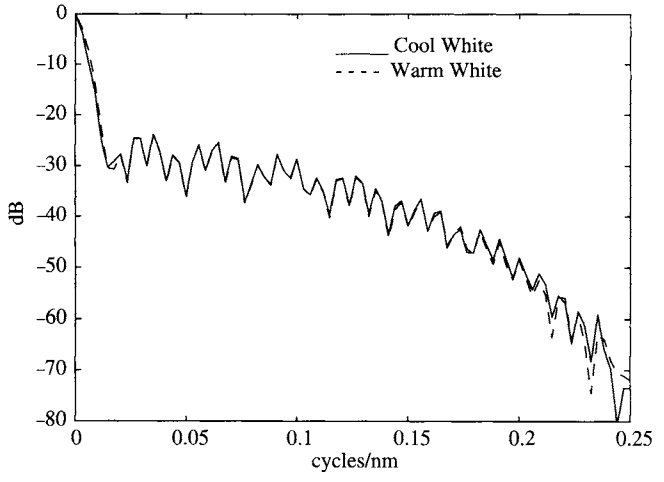

FIGURE 10 Power spectra of cool white fluorescent and warm white fluorescent.

It is with the fluorescent lamps that the 2 nm sampling becomes suspect. The peaks that are seen in the wavelength spectra are characteristic of mercury and are delta function signals at 404.7 nm, 435.8 nm, 546.1 nm and 578.4 nm. The fluorescent lamp can be modeled as the sum of a smoothly varying signal and a delta function series:

$$l(\lambda) = l_d(\lambda) + \sum_{k=1}^{q} \alpha_k \delta(\lambda - \lambda_k) \tag{42}$$

where α_k represents the strength of the spectral line at wavelength λ_k. The wavelength spectra of the phosphors is relatively smooth as seen from Fig. 9.

It is clear that the fluorescent signals are not bandlimited in the sense used previously. The amount of power outside of the band is a function of the positions and strengths of the line spectra. Since the lines occur at known wavelengths, it remains only to estimate their power. This can be done by signal restoration methods which can use the information about this specific signal. Using such methods, the frequency spectrum of the lamp may be estimated by combining the frequency spectra of its components

$$L(\omega) = L_d(\omega) + \sum_{k=1}^{q} \alpha_k e^{j\omega(\lambda_0 - \lambda_k)} \tag{43}$$

where λ_0 is an arbitrary origin in the wavelength domain. The bandlimited spectra $L_d(\omega)$ can be obtained from the sampled restoration and is easily represented by 2 nm sampling.

7 Color I/O Device Calibration

In Section 2, we briefly discussed control of gray scale output. Here, a more formal approach to output calibration will be given. This can be applied to monochrome images by considering only a single band, corresponding to the CIE Y channel. In order to mathematically describe color output calibration, we need to consider the relationships between the color spaces defined by the output device control values and the colorimetric space defined by the CIE.

7.1 Calibration Definitions and Terminology

A *device independent color space* is defined as any space that has a one-to-one mapping onto the CIE XYZ color space. Examples of CIE device independent color spaces include XYZ, Lab, Luv, and Yxy. Current image format standards, such as JPEG, support the description of color in Lab. By definition, a *device dependent color space* cannot have a one-to-one mapping onto the CIE XYZ color space. In the case of a recording device (e.g., scanners), the device dependent values describe the response of that particular device to color. For a

reproduction device (e.g., printers), the device dependent values describe only those colors the device can produce.

The use of device dependent descriptions of color presents a problem in the world of networked computers and printers. A single RGB or CMYK vector can result in different colors on different display devices. Transferring images colorimetrically between multiple monitors and printers with device dependent descriptions is difficult since the user must know the characteristics of the device for which the original image is defined, in addition to those of the display device.

It is more efficient to define images in terms of a CIE color space and then transform this data to device dependent descriptors for the display device. The advantage of this approach is that the same image data is easily ported to a variety of devices. To do this, it is necessary to determine a mapping, $\mathcal{F}_{device}(\cdot)$, from device dependent control values to a CIE color space.

A compromise to using the complicated transformation to a device independent space is to use a *pseudo-device dependent space*. Such spaces provide some degree of matching across input and output devices since "standard" device characteristics have been defined by the color science community. These spaces, which include, sRGB and Kodak's PhotoYCC space, are well defined in terms of a device independent space. As such, a device manufacturer can design an input or output device such that when given sRGB values the proper device independent color value is displayed. However, there do exist limitations with this approach such as non-uniformity and limited gamut.

Modern printers and display devices are limited in the colors they can produce. This limited set of colors is defined as the *gamut* of the device. If Ω_{cie} is the range of values in the selected CIE color space and Ω_{print} is the range of the device control values then the set

$$G = \{\, \mathbf{t} \in \Omega_{cie} \mid \text{there exists } \mathbf{c} \in \Omega_{print} \text{ where } \mathcal{F}_{device}(\mathbf{c}) = \mathbf{t} \,\}$$

defines the gamut of the color output device. For colors in the gamut, there will exist a mapping between the device dependent control values and the CIE XYZ color space. Colors which are in the complement, G^c, cannot be reproduced and must be *gamut-mapped* to a color which is within G. The gamut mapping algorithm $\mathcal{D}$ is a mapping from Ω_{cie} to G, that is $\mathcal{D}(\mathbf{t}) \in G \quad \forall \mathbf{t} \in \Omega_{cie}$. A more detailed discussion of gamut mapping is found in [31].

The mappings $\mathcal{F}_{device}$, $\mathcal{F}^{-1}_{device}$, and $\mathcal{D}$ make up what is defined as a *device profile*. These mappings describe how to transform between a CIE color space and the device control values. The International Color Commission (ICC) has suggested a standard format for describing a profile. This standard profile can be based on a physical model (common for monitors) or a look-up-table (LUT) (common for printers and scanners) [27]. In the next sections, we will mathematically discuss the problem of creating a profile.

7.2 CRT Calibration

A monitor is often used to provide a preview for the printing process, as well as comparison of image processing methods. Monitor calibration is almost always based on a physical model of the device [18, 19, 20]. A typical model is

$$r' = (r - r_0)/(r_{max} - r_0)^{\gamma_r}$$

$$g' = (g - g_0)/(g_{max} - g_0)^{\gamma_g}$$

$$b' = (b - b_0)/(b_{max} - b_0)^{\gamma_b}$$

$$\mathbf{t} = \mathbf{H}[r', g', b']^T$$

where $\mathbf{t}$ is the CIE value produced by driving the monitor with control value $\mathbf{c} = [r, g, b]^T$. The value of the tristimulus vector is obtained using a colorimeter or spectrophotometer.

Creating a profile for a monitor involves the determination of these parameters where r_{max}, g_{max}, b_{max} are the maximum values of the control values (e.g. 255). To determine the parameters, a series of color patches is displayed on the CRT and measured with a colorimeter which will provide pairs of CIE values $\{\mathbf{t}_k\}$ and control values $\{\mathbf{c}_k\}$ $k = 1, \ldots, M$.

Values for γ_r, γ_g, γ_b, r_0, g_0, and b_0 are determined such that the elements of $[r', g', b']$ are linear with respect to the elements of XYZ and scaled between the range [0,1]. The matrix $\mathbf{H}$ is then determined from the tristimulus values of the CRT phosphors at maximum luminance. Specifically the mapping is given by

$$\begin{bmatrix} X \\ Y \\ Z \end{bmatrix} = \begin{bmatrix} X_{Rmax} & X_{Rmax} & X_{Rmax} \\ Y_{Gmax} & Y_{Gmax} & Y_{Gmax} \\ Z_{Bmax} & Z_{Bmax} & Z_{Bmax} \end{bmatrix} \begin{bmatrix} r' \\ b' \\ g' \end{bmatrix}$$

where $[X_{Rmax} Y_{Rmax} Z_{Rmax}]^T$ is the CIE XYZ tristimulus value of the red phosphor for control value $\mathbf{c} = [r_{max}, 0, 0]^T$.

This standard model is often used to provide an approximation to the mapping $\mathcal{F}_{monitor}(\mathbf{c}) = \mathbf{t}$. Problems such as spatial variation of the screen or electron gun dependence are typically ignored. A LUT can also be used for the monitor profile in a manner similar to that described below for the scanner calibration.

7.3 Scanners and Cameras

Mathematically, the recording process of a scanner or camera can be expressed as

$$\mathbf{z}_i = \mathcal{H}(\mathbf{M}^T \mathbf{r}_i)$$

where the matrix $\mathbf{M}$ contains the spectral sensitivity (including the scanner illuminant) of the three (or more) bands of the

device, $\mathbf{r}_i$ is the spectral reflectance at spatial point i, $\mathcal{H}$ models any nonlinearities in the scanner (invertible in the range of interest), and $\mathbf{z}_i$ is the vector of recorded values.

We define *colorimetric recording* as the process of recording an image such that the CIE values of the image can be recovered from the recorded data. This reflects the requirements of ideal sampling in Section 5.4. Given such a scanner, the calibration problem is to determine the continuous mapping $\mathcal{F}_{scan}$ which will transform the recorded values to a CIE color space:

$$\mathbf{t} = \mathbf{A}^T\mathbf{L}\mathbf{r} = \mathcal{F}_{scan}(\mathbf{z}) \text{ for all } \mathbf{r} \in \Omega_r.$$

Unfortunately, most scanners and especially desktop scanners are not colorimetric. This is caused by physical limitations on the scanner illuminants and filters which prevent them from being within a linear transformation of the CIE color matching functions. Work related to designing optimal approximations is found in [28, 29].

For the noncolorimetric scanner, there will exist spectral reflectances which look different to the standard human observer but when scanned produce the same recorded values. These colors are defined as being metameric to the scanner. This cannot be corrected by any transformation $\mathcal{F}_{scan}$.

Fortunately, there will always (except for degenerate cases) exist a set of reflectance spectra over which a transformation from scan values to CIE XYZ values will exist. Such a set can be expressed mathematically as

$$B_{scan} = \{ \mathbf{r} \in \Omega_r \mid \mathcal{F}_{scan}(\mathcal{H}(\mathbf{Mr})) = \mathbf{A}^T\mathbf{Lr} \}$$

where $\mathcal{F}_{scan}$ is the transformation from scanned values to colorimetric descriptors for the set of reflectance spectra in B_{scan}. This is a restriction to a set of reflectance spectra over which the continuous mapping $\mathcal{F}_{scan}$ exists.

Look-up-tables, neural nets, nonlinear and linear models for $\mathcal{F}_{scan}$ have been used to calibrate color scanners [22, 23, 24, 25, 32]. In all of these approaches, the first step is to select a collection of color patches which span the colors of interest. These colors should not be metameric to the scanner or to the standard observer under the viewing illuminant. This constraint assures a one-to-one mapping between the scan values and the device independent values across these samples. In practice, this constraint is easily obtained. The reflectance spectra of these M_q color patches will be denoted by $\{\mathbf{q}\}_k$ for $1 \le k \le M_q$.

These patches are measured using a spectrophotometer or a colorimeter which will provide the device independent values

$$\{\mathbf{t}_k = \mathbf{A}^T\mathbf{q}_k\} \quad \text{for} \quad 1 \le k \le M_q.$$

Without loss of generality, $\{\mathbf{t}_k\}$ could represent any colorimetric or device independent values, e.g., CIELAB, CIELUV in which case $\{\mathbf{t}_k = \mathcal{L}(\mathbf{A}^T\mathbf{q}_k)\}$ where $\mathcal{L}(\cdot)$ is the transformation from CIEXYZ to the appropriate color space. The patches are also measured with the scanner to be calibrated providing $\{\mathbf{z}_k = \mathcal{H}(\mathbf{M}^T\mathbf{q}_k)\}$ for $1 \le k \le M_q$. Mathematically, the calibration problem is: find a transformation $\mathcal{F}_{scan}$ where

$$\mathcal{F}_{scan} = \arg(\min_{\mathcal{F}} \sum_{i=1}^{M_q} ||\mathcal{F}(\mathbf{z}_i) - \mathbf{t}_i||^2)$$

and $||.||^2$ is the error metric in the CIE color space. In practice, it may be necessary and desirable to incorporate constraints on $\mathcal{F}_{scan}$ [31].

7.4 Printers

Printer calibration is difficult due to the nonlinearity of the printing process, and the wide variety of methods used for color printing (e.g., lithography, inkjet, dye sublimation etc.). Thus, printing devices are often calibrated with an LUT with the continuum of values found by interpolating between points in the LUT [22, 26].

To produce a profile of a printer, a subset of values spanning the space of allowable control values, $\mathbf{c}_k$ for $1 \le k \le M_p$, for the printer is first selected. These values produce a set of reflectance spectra which are denoted by $\mathbf{p}_k$ for $1 \le k \le M_p$.

The patches $\mathbf{p}_k$ are measured using a colorimetric device which provides the values

$$\{\mathbf{t}_k = \mathbf{A}^T\mathbf{p}_k\} \quad \text{for} \quad 1 \le k \le M_p$$

The problem is then to determine a mapping $\mathcal{F}_{print}$ which is the solution to the optimization problem

$$\mathcal{F}_{print} = \arg(\min_{\mathcal{F}} \sum_{i=1}^{M_p} ||\mathcal{F}(\mathbf{c}_i) - \mathbf{t}_i||^2)$$

where as in the scanner calibration problem, there may be constraints which $\mathcal{F}_{print}$ must satisfy.

7.5 Calibration Example

Before presenting an example of the need for calibrated scanners and displays, it is necessary to state some problems with the display to be used, i.e., the color printed page. Currently, printers and publishers do not use the CIE values for printing but judge the quality of their prints by subjective methods. Thus, it is impossible to numerically specify the image values to the publisher of this book. We have to rely on the experience of the company to produce images which faithfully reproduce those given them. Every effort has been made to reproduce the images as accurately as possible. The tiff image format allows the specification of CIE values and the images defined by those values can be found on the ftp site,

FIGURE 11 Original Lena. (See color insert.)

FIGURE 13 New scan of Lena. (See color insert.)

ftp.ncsu.edu in directory pub/hjt/calibration. Even in the .tiff format problems arise because of quantization to 8 bits.

The original color Lena image is available in many places as an RGB image. The problem is that there is no standard to which the RGB channels refer. The image is usually printed to an RGB device (one that takes RGB values as input) with no transformation. An example of this is shown in Fig. 11. This image compares well with current printed versions of this image, e.g., those shown in papers in the special issue on color image processing of the IEEE Transactions on Image Processing [35]. However, the displayed image does not compare favorably with the original. An original copy of the image was obtained and scanned using a calibrated scanner and then printed using a calibrated printer. The result, shown in Fig. 12, does compare well with the original. Even with the display problem mentioned above, it is clear that the images are sufficiently different to make the point that calibration is necessary for accurate comparisons of any processing method that uses color images. To complete the comparison, the RGB image that was used to create the corrected image shown in Fig. 12, was also printed directly on the RGB printer. The result shown in Fig. 13, further demonstrates the need for calibration. A complete discussion of this calibration experiment is found in [31].

FIGURE 12 Calibrated Lena. (See color insert.)

8 Summary and Future Outlook

The major portion of the chapter emphasized the problems and differences in treating the color dimension of image data. Understanding of the basics of uniform sampling is required to proceed to the problems of sampling the color component. The phenomenon of aliasing is generalized to color sampling by noting that the goal of most color sampling is to reproduce the sensation of color and not the actual color spectrum. The calibration of recording and display devices is required for accurate representation of images. The proper recording and display outlined in Section 7 cannot be overemphasized.

While the fundamentals image recording and display are well understood by experts in that area, they are not well appreciated by the general image processing community. It is hoped that future work will help widen the understanding of this aspect of image processing. At present, it is fairly difficult to calibrate color image I/O devices. The interface between the devices and the interpretation of the data is still problematic. Future work can make it easier for the average user to obtain, process and display accurate color images.

Acknowledgment

The author would like to acknowledge Michael Vrhel for his contribution to the section on color calibration. Most of the material in that section was the result of a joint paper with him [31].

References

[1] MATLAB, High Performance Numeric Computation and Visualization Software, The Mathworks Inc., 24 Prime Park Way, Natick, MA 01760.

[2] A. V. Oppenheim and R. W. Schafer, *Discrete-Time Signal Processing.* (Prentice-Hall, 1989).

[3] D. E. Dudgeon and R. M. Mersereau, *Multidimensional Digital Signal Processing.* (Prentice-Hall, 1984).

[4] H. B. Barlow and J. D. Mollon, *The Senses.* (Cambridge University Press, Cambridge, U.K., 1982).

[5] J. B. Cohen and W. E. Kappauf, "Metameric color stimuli, fundamental metamers, and Wyszecki's metameric blacks," *Am. J. of Psychology*, 95(4), 537–564, Winter 1982.

[6] H. Grassmann, "Zur therorie der Farbenmischung," *Annalen der Physik und Chemie*, 89, 69–84, 1853.

[7] H. Grassmann, "On the theory of compound colours," *Philos. Mag.*, 7(4), 254–264, 1854.

[8] B. K. P. Horn, "Exact reproduction of colored images," *Computer Vision, Graph. and Image Proc.*, 26, 135–167, 1984.

[9] A. K. Jain, *Fundamentals of Digital Image Processing.* (Prentice-Hall, Englewood Cliffs, N.J., 1989).

[10] H. J. Trussell and M. S. Kulkarni, "Sampling and processing of color signals," *IEEE Trans. Image Proc.*, 5(4), 677–681, April 1996.

[11] D. L. MacAdam, "Visual sensitivities to color differences in daylight," *J. Opt. Soc. Am.*, 32(5), 247–274, May 1942.

[12] H. J. Trussell, "Application of set theoretic methods to color systems," *Color: Res. and Appl.*, 16(1), 31–41, Feb. 1991.

[13] P. L. Vora and H. J. Trussell, "Measure of goodness of a set of colour scanning filters," *J. Optical Soc. of Am.*, 10(7), 1499–1508, July 1993.

[14] B. A. Wandell, "The synthesis and analysis of color images," *IEEE Trans. Patt. Anal. and Mach. Intel.*, PAMI-9(1), 2–13, Jan. 1987.

[15] B. A. Wandell, *Foundations of Vision.* (Sinauer Assoc. Inc, Sunderland, MA, 1995).

[16] G. Wyszecki and G. H. Felder, "New color matching ellipses," *J. Opt. Soc. Am.* 62, 1501–1513, 1971.

[17] G. Wyszecki and W. S. Stiles, *Color Science: Concepts and Methods, Quantitative Data and Formulae*, 2nd Ed., John Wiley and Sons, New York, NY, 1982.

[18] W. B. Cowan, "An inexpensive scheme for calibration of a color monitor in terms of standard CIE coordinates," *Comput. Graph.*, 17, 315–321, July 1983.

[19] R. S. Berns, R. J. Motta, and M. E. Grozynski, "CRT colorimetry. Part I: Theory and practice," *Color Res. Appl.*, 18, 5–39, Feb. 1988.

[20] R. S. Berns, R. J. Motta, and M. E. Grozynski, "CRT colorimetry. Part II: Metrology," *Color Res. Appl.*, 18, 315–325, Feb. 1988.

[21] M. J. Vrhel, R. Gershon, and L. S. Iwan, "Measurement and analysis of object reflectance spectra," *Color Res. Appl.*, 19, 4–9, Feb. 1994.

[22] P. C. Hung, "Colorimetric calibration in electronic imaging devices using a look-up table model and interpolations," *J. Electronic Imaging*, 2, 53–61, Jan. 1993.

[23] H. R. Kang and P. G. Anderson, "Neural network applications to the color scanner and printer calibrations," *J. Electronic Imaging*, 1, 125–134, April 1992.

[24] H. Haneishi, T. Hirao, A. Shimazu, and Y. Mikaye, "Colorimetric precision in scanner calibration using matrices," in *Proc. Third IST/SID* & Color Imaging Conference: Color Science, Systems and Applications, Nov. 1995, 106–108.

[25] H. R. Kang, "Color scanner calibration," *J. Imaging Sci. Technol.*, 36, 162–170, Mar./Apr. 1992.

[26] J. Z. Chang, J. P. Allebach, and C. A. Bouman, "Sequential linear interpolation of multidimensional functions," *IEEE Transactions on Image Processing*, 6(9), 1231–1245, Sept. 1997.

[27] International Color Consortium, *Int. Color Consort. Profile Format Ver. 3.4*, available at http://color.org/.

[28] P. L. Vora and H. J. Trussell, "Mathematical methods for the design of color scanning filters," *IEEE Trans. Image Proc.* IP-6(2), 312–320, Feb. 1997.

[29] G. Sharma, H. J. Trussell, and M. J. Vrhel, "Optimal nonnegative color scanning filters," *IEEE Trans. Image Proc.*, 7(1), 129–133, Jan 1998.

[30] M. J. Vrhel, and H. J. Trussell, "Optimal color filters in the presence of noise," *IEEE Trans. Image Proc.*, 4(6), 814–823, June 1995.

[31] M. J. Vrhel, and H. J. Trussell, "Color device calibration: a mathematical formulation," *IEEE Trans. Image Proc.*, in press 1999.

[32] M. J. Vrhel, and H. J. Trussell, "Color scanner calibration via neural networks," Proc. Conf. on Acous., Speech and Sig. Proc., March 15–19, 1999, Phoenix, AZ.

[33] N. P. Galatsanos, and R. T. Chin, "Digital restoration of multichannel images," *IEEE Trans. Acous., Speech and Sig. Proc.*, Vol ASSP-37(3), 415–421, Mar. 1989.

[34] CIE, "Industrial colour difference evaluation," Technical Report 116–1995, 1995.

[35] *IEEE Trans. Image Proc.*, 6(7), July 1997.

FIGURE 4.6.11 Original Lena.

FIGURE 4.6.12 Calibrated Lena.

FIGURE 4.6.13 New scan of Lena.

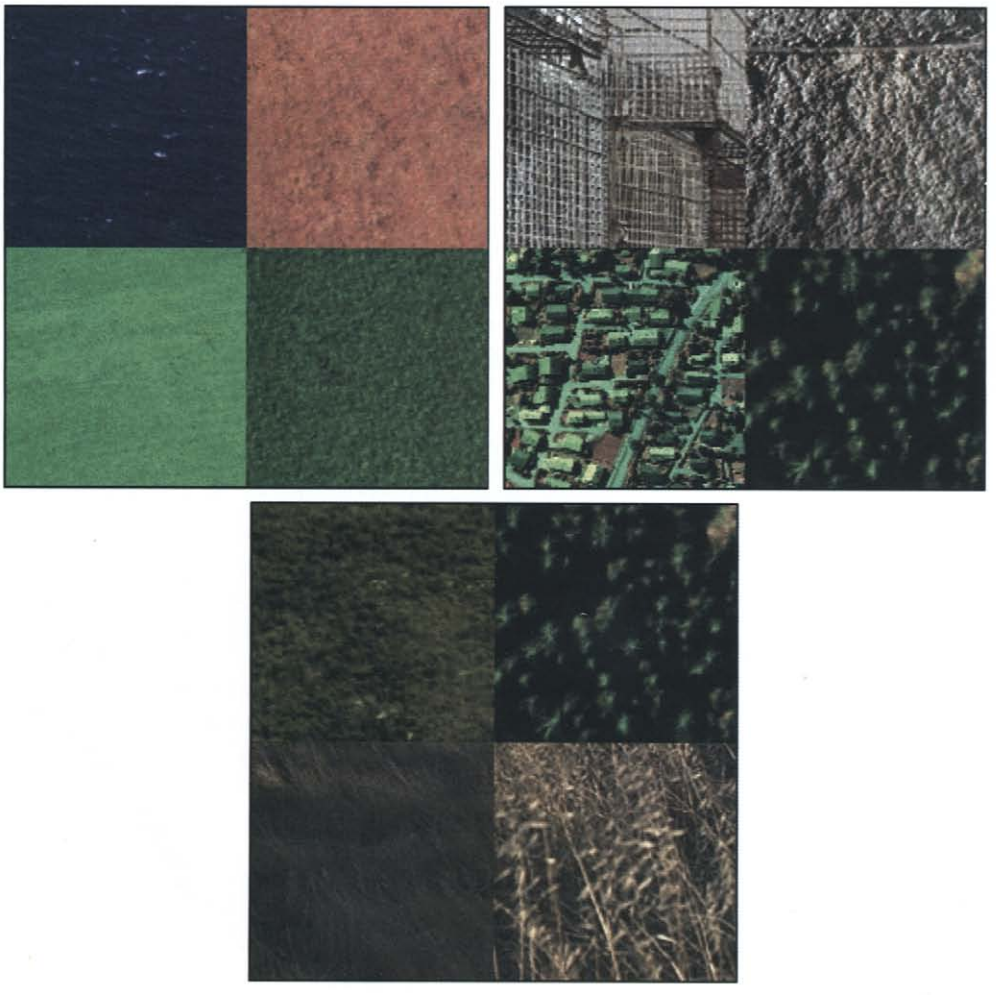

FIGURE 4.8.2 Collection of images; in each there are four clearly distinguishable segments.